


Article

# Product Inhibition of Biological Hydrogen Production in Batch Reactors

Subhashis Das <sup>1,\*</sup> , Rajnish Kaur Calay <sup>1</sup>, Ranjana Chowdhury <sup>2</sup>, Kaustav Nath <sup>3</sup> and Fasil Ejigu Eregno <sup>1</sup>

<sup>1</sup> Faculty of Engineering Science and Technology, UiT-The Arctic University of Norway, 8514 Narvik, Norway; rajnish.k.calay@uit.no (R.K.C.); fasil.e.eregno@uit.no (F.E.E.)

<sup>2</sup> Department of Chemical Engineering, Jadavpur University, Kolkata 700032, India; ranjana.juchem@gmail.com

<sup>3</sup> Department of Biotechnology, Indian Institute of Technology, Kharagpur 721302, India; knstar.nath8@gmail.com

\* Correspondence: das.subhashis@gmail.com or subhashis.das@uit.no

Received: 20 February 2020; Accepted: 10 March 2020; Published: 12 March 2020



**Abstract:** In this paper, the inhibitory effects of added hydrogen in reactor headspace on fermentative hydrogen production from acidogenesis of glucose by a bacterium, *Clostridium acetobutylicum*, was investigated experimentally in a batch reactor. It was observed that hydrogen itself became an acute inhibitor of hydrogen production if it accumulated excessively in the reactor headspace. A mathematical model to simulate and predict biological hydrogen production process was developed. The Monod model, which is a simple growth model, was modified to take inhibition kinetics on microbial growth into account. The modified model was then used to investigate the effect of hydrogen concentration on microbial growth and production rate of hydrogen. The inhibition was moderate as hydrogen concentration increased from 10% to 30% (*v/v*). However, a strong inhibition in microbial growth and hydrogen production rate was observed as the addition of H<sub>2</sub> increased from 30% to 40% (*v/v*). Practically, an extended lag in microbial growth and considerably low hydrogen production rate were detected when 50% (*v/v*) of the reactor headspace was filled with hydrogen. The maximum specific growth rate ( $\mu_{\max}$ ), substrate saturation constant (*K<sub>s</sub>*), a critical hydrogen concentration at which microbial growth ceased (H<sub>2</sub><sup>\*</sup>) and degree of inhibition were found to be 0.976 h<sup>-1</sup>, 0.63 ± 0.01 gL, 24.74 mM, and 0.4786, respectively.

**Keywords:** hydrogen; reactor headspace; product inhibition; kinetic modelling; *clostridium acetobutylicum*

## 1. Introduction

Hydrogen energy is considered one of the most promising energy storage hubs and carriers of energy harvested from renewable energy sources. Hydrogen fuel cell technology, particularly, has the potential to replace fossil fuel-based internal combustion engine mainly used in the transport sector [1]. Hydrogen is the most abundant element, but it does not exist in its molecular form and has to be produced using different technologies, such as by electrolysis from water, steam reforming, and gasification of fossil fuel. All of these technologies are energy-intensive. For example, 1 kg of hydrogen (specific energy of 40 kWh/kg) requires 50–55 kWh of electricity by electrolysis of water, which is 70–80% efficient. Therefore, exploring energy-efficient hydrogen production methods from renewable sources are necessary. Biological and thermochemical processes can convert various types of biomass such as agriculture, forest sector, and bio-waste directly into hydrogen. Biological processes for hydrogen production are more environment-friendly and consume less energy compared to

thermochemical processes [2]. When using bio-waste, the production of hydrogen becomes even more cost-effective due to the utilization of low-cost waste biomass as feedstock.

The available paths of biohydrogen are typically categorized as either photo fermentation (PF) or dark fermentation (DF). PF is carried out by nonoxygenic photosynthetic bacteria, which use sunlight and biomass to produce hydrogen. DF, however, takes place under anaerobic conditions. Carbohydrate-rich biomasses, along with industrial wastes, can be used as the feedstock of DF for hydrogen production [3]. The yield of hydrogen is higher in the PF process, although there are studies [4–7] that establish that treatment capacity of organic waste and hydrogen production rate of DF is better than the PF.

Considering the potential of DF, a detailed investigation is required for scaling up the technology into industrial scale. The most critical issue that needs to be addressed is increasing the production of hydrogen, which depends on the activity of microorganisms. Production of hydrogen quantitatively and qualitatively strongly depend on the metabolic pathway of microorganisms. The metabolic pathway of microorganism in DF often deviates due to the influence of certain physicochemical parameters such as substrate composition, culture pH, or concentration of byproducts of reaction medium. On the other hand, there are various research studies [7–14] that have identified the dark fermentation process parameters that influence the production of hydrogen, such as the optimal functionality of the microorganisms, hydraulic retention time, temperature, and the partial pressure of hydrogen of reaction processes. Therefore, it is possible to enrich hydrogen productivity by improving approaches to metabolic pathway control.

The primary pathway in the dark fermentation is the breakdown of carbohydrate-rich substrates to  $H_2$  and other intermediate products such as volatile fatty acids (VFAs) and alcohols by the use of bacteria. There are a few kinds of anaerobic mesophilic or thermophilic bacteria such as genus *Clostridium*, which can produce hydrogen at a high rate, in the course of their metabolism. During fermentative hydrogen production, polysaccharides are hydrolyzed into simpler saccharides. These simpler sugars are easily taken up by hydrogen-producing bacteria (HPB) and enter the ‘Embden-Meyerhof-Parnas’ pathway to produce pyruvate and nicotinamide adenine dinucleotide (NADH). NADH becomes  $NAD^+$  by donating electrons to the electron transport chain and  $H^+$  is transported across the membrane. The major products are further formed from pyruvate and these are mainly short-chain fatty acids (e.g., acetate, butyrate, lactate) as well as alcohols (e.g., butanol, ethanol). Among these products, lactate, butanol, and ethanol have the only contribution to re-oxidized NADH. As the reactions proceed,  $CO_2$  formed from other metabolic reactions and increases its concentration in the liquid medium. The excess  $CO_2$  in liquid culture reacts with pyruvate using NADH to produce succinate and oxidize NADH by reducing  $H^+$ . The product formation from pyruvate is shown in Figure 1.

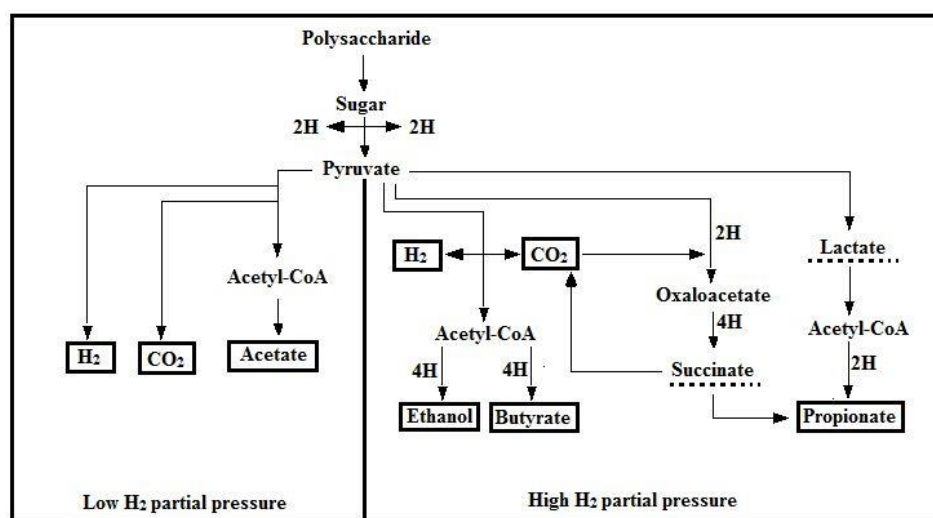


Figure 1. Metabolic pathway of  $H_2$  formation.

On the other hand, hydrogenase, an enzyme that catalyzes the reversible oxidation of molecular hydrogen during fermentative hydrogen production, is often affected by the H<sub>2</sub> concentration in liquid culture. At higher H<sub>2</sub> partial pressure in liquid broth, the reduction of ferredoxin, which mediates electron transfer, takes place and the reduction of a proton to H<sub>2</sub> becomes thermodynamically less favourable, which results in a reduction of H<sub>2</sub> formation.

Numerous research articles have shown the inhibitory effects of hydrogen concentration in terms of partial pressure in the reactor [7–9] and these articles explain how to overcome these inhibitory effects to improve H<sub>2</sub> productivity. On the way to decrease partial pressure to improve H<sub>2</sub> productivity, several strategies were employed such as continuous gas release [6–8], larger headspace volume [9], vacuum stripping [13], or sparging with an inert gas like N<sub>2</sub> or CO<sub>2</sub> [15,16].

Different kinetic models describe the fermentation process of hydrogen production [17–19]. These models depend on physicochemical parameters and microbial environment within the reactor. Usually, these models are developed considering the effects of substrate concentration, pH, and temperature on the hydrogen production process. Kinetic models are also used to design reactors and provide proper information to adopt control strategies for hydrogen production processes. On the other hand, kinetic models are useful to describe the inhibitory effects of substrate, temperature, pH, dilution rate (in case of the continuous process), and soluble metabolites, which are generated during DF [18]. However, models that describe the effects of hydrogen accumulated in the headspace of a batch reactor on microbial growth and hydrogen production are limited. Therefore, the present study investigates the influence of hydrogen on microbial growth and evaluates how the produced hydrogen hinders the rate of production of hydrogen. The main aim of the study is to experimentally examine the adverse of produced hydrogen on microbial growth and adopted mathematical models to predict the production rate hydrogen batch reactors.

## 2. Materials and Methods

In order to achieve the objective, first, a series of experiments were performed in a batch reactor. A hydrogen-producing bacterium *Clostridium acetobutylicum*, which is strictly anaerobic, was selected in the present study where glucose was the sole nutrient for microbial growth. In the batch reactor operation, the headspace gas concentration, and the nutrient concentration, were varied to observe the effect of hydrogen, accumulated in the headspace on microbial growth and hydrogen production rate. Observing the nature of the batch reaction suitable microbial reaction kinetics was adopted secondly. Furthermore, the kinetic parameters were determined by using experimental data. The experimental procedure is described below.

### 2.1. Experiments

#### 2.1.1. Inoculum

A pure lyophilized strain of *Clostridium Acetobutylicum* (NCIM 2337) was procured from National chemical laboratory (NCL), Pune, India. Cooked meat (CM) medium containing beef extract 45 g/L, glucose 2 g/L, peptone 20 g/L, NaCl 5 g/L was used for the growth of lyophilized bacterial culture at 37 °C for 72 h.

#### 2.1.2. Reactor Setup for Batch Experiment

Batch experiments were conducted in 250 mL cork fitted Erlenmeyer flask having an outlet port at the bottom. A cork was fitted to a glass tube and connected to a gas measuring tube for gas sampling. The batch experimental setup is shown in Figure 2a and the whole system is presented schematically in Figure 2b.

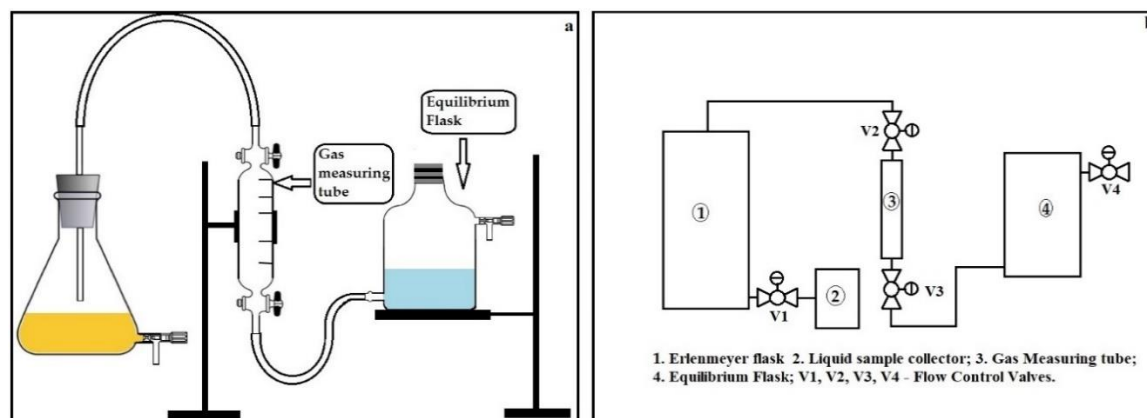


**Figure 2.** Experimental setup for batch test (a); schematic diagram of the experimental setup (b).

An Erlenmeyer flask was half filled with the CM medium along with 1% (*v/v*) of inoculum into the medium then remaining void was filled completely with the CM medium. The flask was then firmly sealed with the cork and 150 mL of argon gas was passed through the flask by a glass tube for displacing the CM media from the bottom of the flask. Thus, the flask was left with 100 mL of CM medium with bacterial culture and 150 mL headspace was occupied by a mixture of argon and hydrogen. The whole setup was then kept in the incubator at maintaining the temperature of 37 °C and pH of 7.2, which are the ideal conditions for this bacteria. Initial hydrogen concentration in the reactor headspace were varied in the range of 0% (*v/v*) to 50% (*v/v*). Initially, H<sub>2</sub> experiments were performed by varying glucose concentration of the modified CM medium in the range of 2 g/L to 5 g/L. At each initial substrate concentration, microbial growth pattern was observed for 30 h. An interval of 3 h samples were collected. The produced gas was accumulated in the reactor headspace and was taken out from the flask using a gas sampling tube, connected with the flask for examining the gas composition after each interval. Each experimental run was repeated three times to ensure the repeatability and the statistical accuracy of the results.

### 2.1.3. Sample Collection and Analysis

The biomass concentration of each sample was determined in terms of optical density with a spectrophotometer at 600 nm wavelength. Each liquid sample was centrifuged at 10,000 rpm and the supernatant was collected in order to find out the reducing sugar concentration using the dinitrosalicylic (DNS) acid reagent [20]. Next, 100 mL of gas was collected after every 3 h interval from the headspace of batch reactor using a gas sampling tube. Collected gas was then passed through an ORSAT apparatus for the removal of CO<sub>2</sub> gas present in the gas sample. Furthermore, the remaining gas composition was analyzed by gas chromatography. On a molecular sieve column (13×, 180 cm by 1/4 inch, 60–80 mesh), the gases were separated where argon was the carrier gas at 100 °C. A 406 Packard GC equipped with a thermal conductivity detector (TCD, 100 mA) was used to measure hydrogen concentration.

### 2.2. Kinetic Modelling

Herein, we consider the Monod model, which is the most popular and simplest model for describing the microbial reaction of microbial growth within a single substrate. The reaction kinetics are expressed as:



the rate of reaction will be:

$$r_c = \frac{dX}{dt} = \frac{\mu_{\max} S}{K_S + S} X \quad (2)$$

where,  $r_c$  is the microbial growth rate, ( $\text{gL}^{-1}\text{h}^{-1}$ );  $X$  is the dry cell concentration, ( $\text{gL}^{-1}$ );  $t$  is time, (h);  $\mu_{\max}$  is the maximum specific growth rate of cells, ( $\text{h}^{-1}$ );  $S$  is the substrate concentration, ( $\text{gL}^{-1}$ ); and  $k_s$  is the Monod constant or substrate saturation constant, ( $\text{gL}^{-1}$ ).

The inhibition in microbial growth occurs typically due to the excess presence of substrate, product, or other inhibitory substance in the cell growth medium. Hans and Levenspiel [21] express the inhibition of microbial growth model as:

$$\frac{dX}{dt} = \mu_{\max} \left(1 - \frac{H_2}{H_2^*}\right)^n \left(\frac{S \cdot X}{S + k_s \left(1 - \frac{X}{X^*}\right)^m}\right) \quad (3)$$

where,  $H_2^*$  is the critical molar concentration of hydrogen at which microbial reaction ceases, (M);  $n$  is the degree of inhibition; and  $m$  is the degree of inhibition.

#### Evaluation of the Constants

Taking inhibition of microbial growth Equation (3) into account, Equation (2) can be expressed as a generalized Monod model:

$$\mu = \frac{\mu_{\max, \text{obs}} \cdot S}{k_{s, \text{obs}} + S} \quad (4)$$

where,  $\mu$  is the specific microbial growth rate ( $\text{h}^{-1}$ ) and  $_{\text{obs}}$  is the experimentally observed value.

$$\mu = \frac{1}{X} \cdot \frac{dX}{dt} \quad (5)$$

$$\mu_{\max, \text{obs}} = \mu_{\max} \left(1 - \frac{H_2}{H_2^*}\right)^n \quad (6)$$

$$k_{s, \text{obs}} = k_s \left(1 - \frac{X}{X^*}\right)^m \quad (7)$$

By reciprocating Equation (4),

$$\frac{1}{\mu} = \frac{k_{s, \text{obs}}}{\mu_{\max, \text{obs}}} \cdot \frac{1}{S} + \frac{1}{\mu_{\max, \text{obs}}} \quad (8)$$

plots of  $1/\mu$  and  $1/S$  can be obtained at each initially added hydrogen in reactor headspace, which is shown in the Figure 3.  $\mu_{\max, \text{obs}}$  and  $k_{s, \text{obs}}$  at each headspace  $H_2$  concentration can be determined by evaluating the intercepts and abscissas on Figure 3.

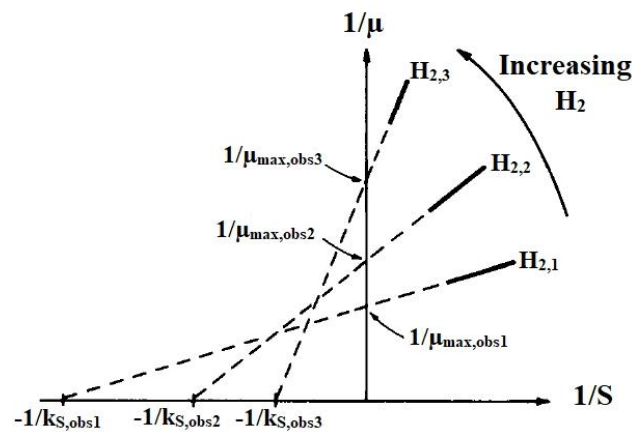


**Figure 3.** Evaluation procedure of  $\mu_{\max,obs}$  and  $k_{s,obs}$  at various concentration of inhibitor; Reproduced with permission from Keehyun Han and Octave Levenspiel, *Biotechnology & Bioengineering*; published by John Wiley and Sons, 2004 [21].

After determining values of  $\mu_{\max,obs}$  and  $k_{s,obs}$  at different headspace  $H_2$  concentration, constants in Equation (3) can be evaluated. On taking logarithms of Equation (5) i.e.,

$$\ln(\mu_{\max,obs}) = n \cdot \ln\left(1 - \frac{H_2}{H_2^*}\right) + \ln(\mu_{\max}) \quad (9)$$

a plot of  $\ln(\mu_{\max,obs})$  and  $\ln(1 - H_2/H_2^*)$  gives the values of  $\mu_{\max}$  and  $n$ . If the values of  $H_2^*$  is not identified from the experiments then a guessed value of  $H_2^*$  have to be considered. A corrected value of  $H_2^*$  can be determined until a straight line is obtained which is shown in Figure 4.

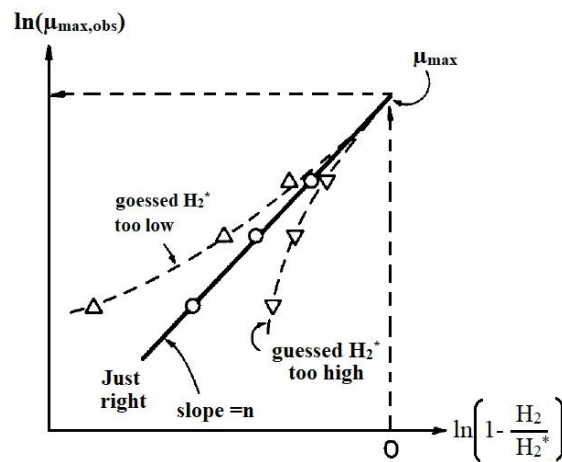


**Figure 4.** Evaluation procedure of  $\mu_{\max}$ ,  $n$  and  $H_2^*$  for product inhibition; Reproduced with permission from Keehyun Han and Octave Levenspiel, *Biotechnology & Bioengineering*; published by John Wiley and Sons, 2004 [21].

### 3. Results

#### 3.1. Effects of Added $H_2$ in the Reactor Headspace

Effects of hydrogen concentration accumulated in the reactor headspace on microbial growth and hydrogen production were studied by conducting experiments in batch reactor. The results were shown in Figures 5–10. In these figures, the time history of biomass concentration and produced hydrogen concentration were showed when initial hydrogen concentration in the reactor headspace

was varied. From these figures, it is clear that microbial growth as well as hydrogen productivity were greatly influenced by the presence of hydrogen in the reactor headspace.

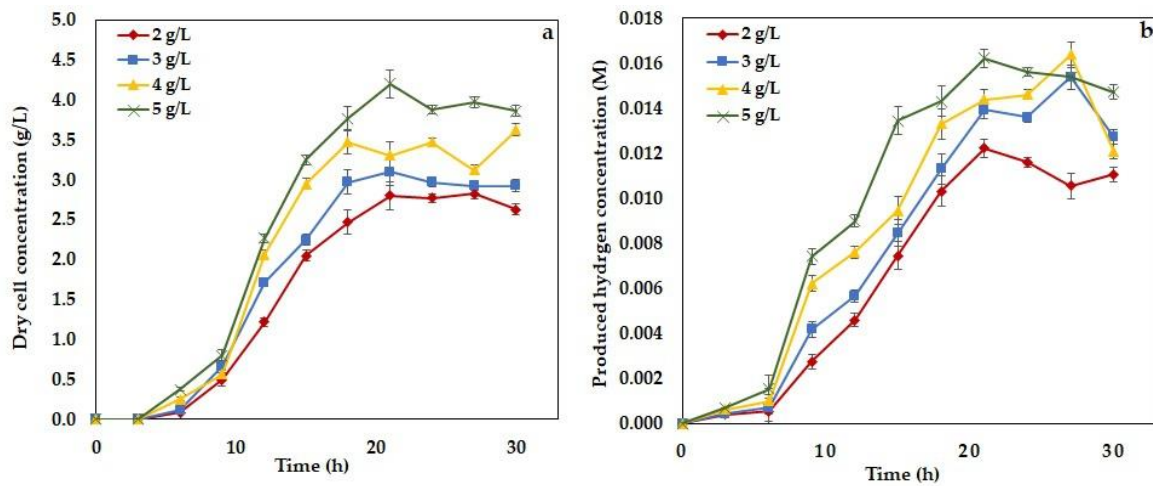


**Figure 5.** Experimental time histories of dry cell concentration (a) and hydrogen concentration (b) with initial 0%  $H_2$  in reactor headspace at different substrate concentration.

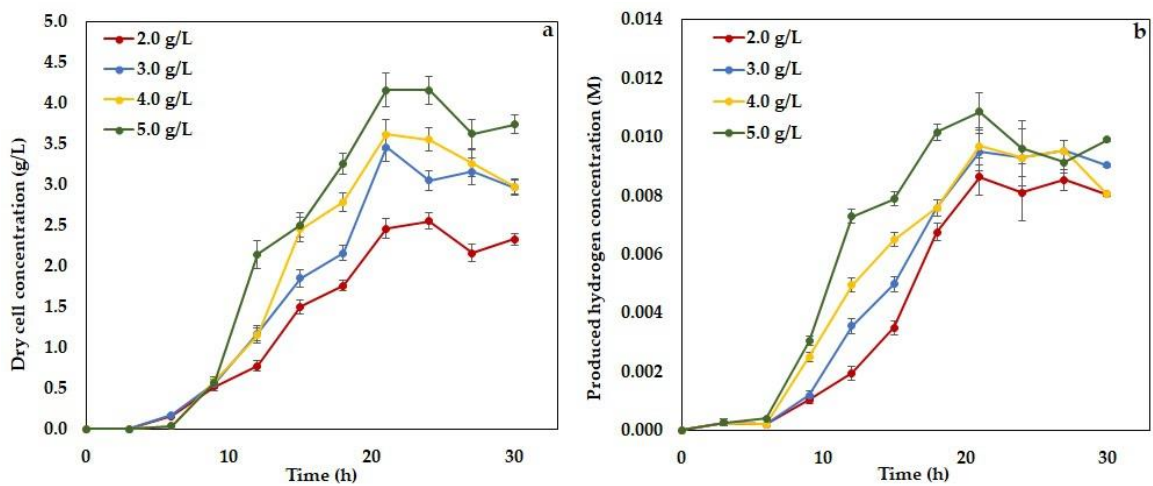


**Figure 6.** Experimental time histories of dry cell concentration (a) and hydrogen concentration (b) with initial 10%  $H_2$  in reactor headspace at different substrate concentration.

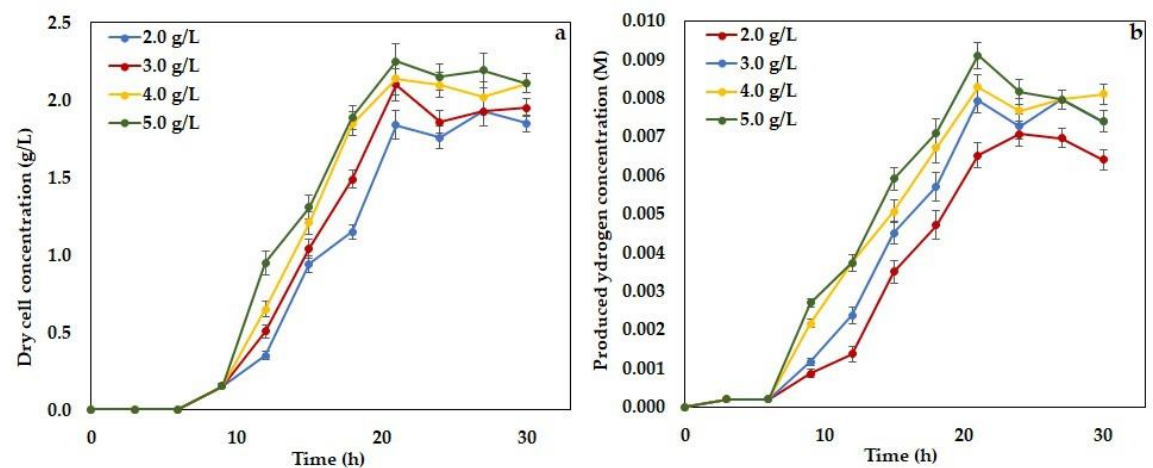


**Figure 7.** Experimental time histories of dry cell concentration (a) and hydrogen concentration (b) with initial 20%  $H_2$  in reactor headspace at different substrate concentration.

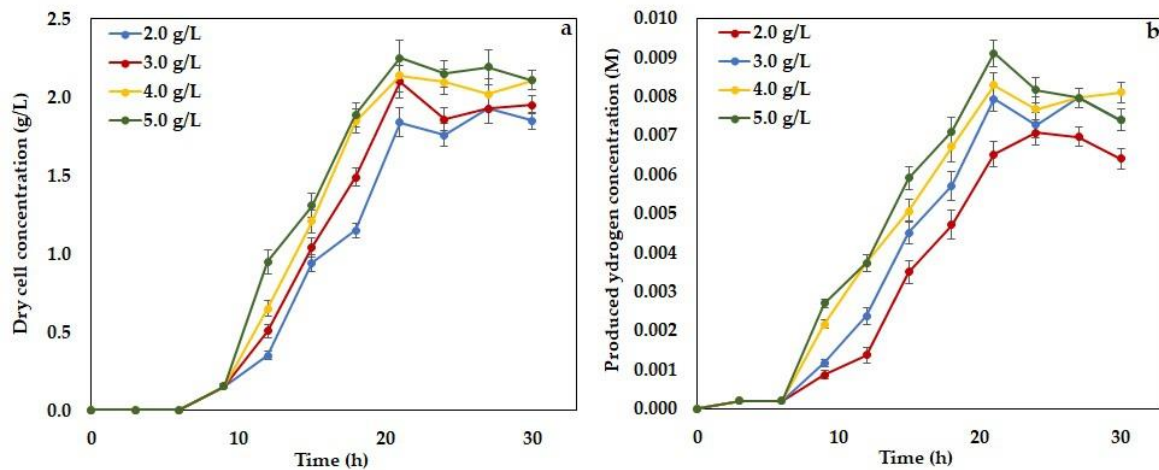


**Figure 8.** Experimental time histories of dry cell concentration (a) and produced hydrogen concentration (b) with initial 30% (*v/v*) H<sub>2</sub> in reactor headspace at different substrate concentration.

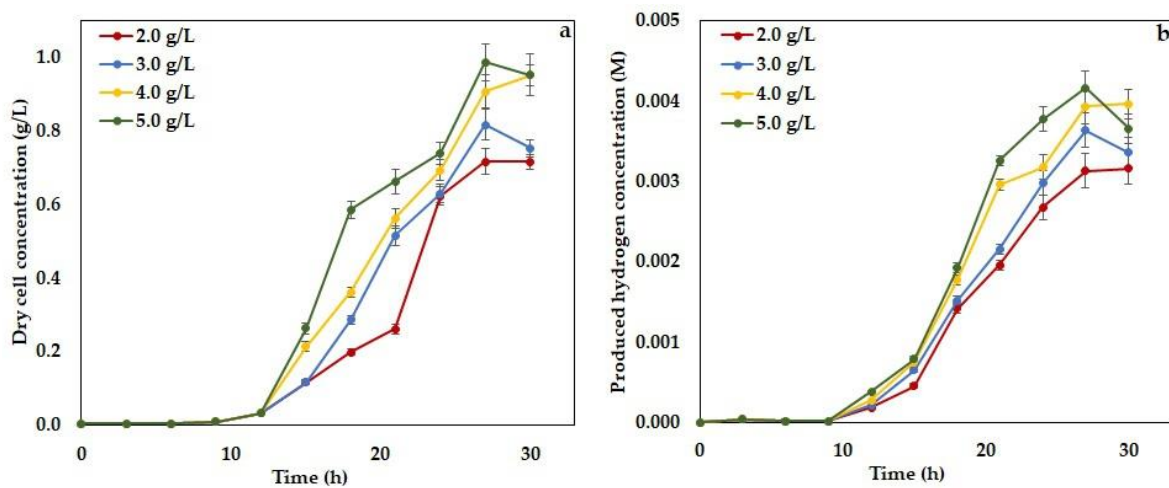


**Figure 9.** Experimental time histories of dry cell concentration (a) and hydrogen concentration (b) with initial 40% H<sub>2</sub> in reactor headspace at different substrate concentration.

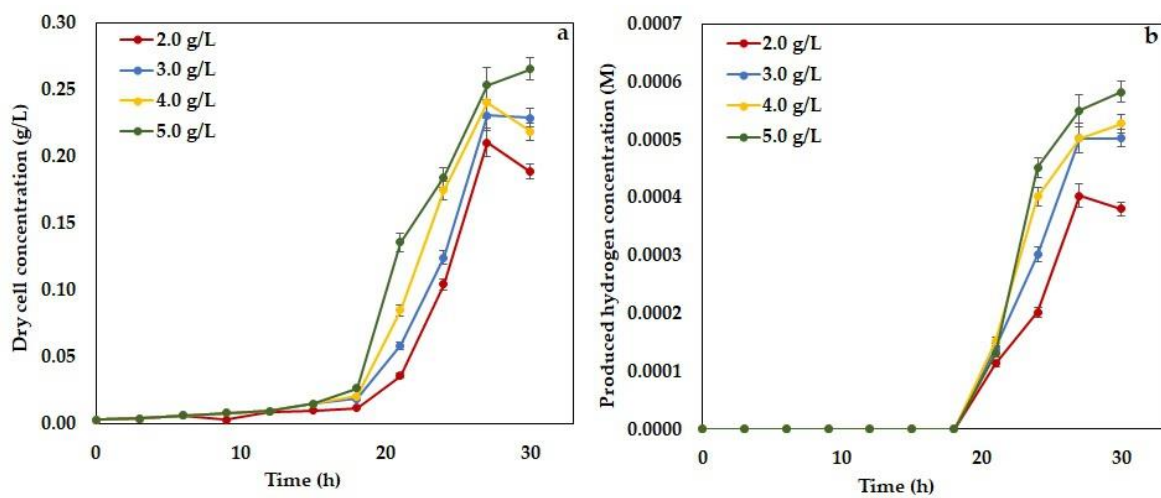


**Figure 10.** Experimental time histories of dry cell concentration (a) and hydrogen concentration (b) with initial 50% H<sub>2</sub> in reactor headspace at different substrate concentration.



Initially, experiments were started when argon gas was present in the reactor headspace and initial glucose concentration in the liquid medium was varied in the range of 2 g/L to 5 g/L. At each variation of glucose, the microbial growth pattern and hydrogen production rate were observed for 30 h. The time histories of microbial growth and hydrogen production rate were presented in Figure 5. From this figure, it is observed that microbial growth, as well as hydrogen production, was started immediately after 3 h of reaction time. There was no significant lag phase of microbial growth detected. A stationary phase was started at 21 h for every initial glucose concentration. The maximum productivity of hydrogen was  $7.81 \text{ mL}^{-1}\text{h}^{-1}$  when initial glucose concentration in the liquid medium was 5 g/L.

On the other hand, when 10% (v/v) of  $\text{H}_2$  added to reactor headspace, microbial growth and hydrogen production started after 6 h of incubation time, which is shown in Figure 6. Although there was no such difference in specific growth and hydrogen production observed for different initial substrate concentration, the maximum hydrogen productivity decreased to  $5.17 \text{ mL}^{-1}\text{h}^{-1}$ , which is comparable to the 0% (v/v) added  $\text{H}_2$  condition. The exponential phase of microbial growth ended at 21 h which was same as the previous condition.

In the case of 20% (v/v) added  $\text{H}_2$  in the reactor headspace, the hydrogen production rate as well as biomass production rate further decreased, which can be observed from Figure 7. In this condition, propagation of hydrogen production and bacterial growth was quite similar to that of 10% (v/v) added  $\text{H}_2$  condition, where microbial growth reached at its exponential phase at 6 h and it extended up to 21 h. However, in this condition, maximum hydrogen productivity decreased to  $4.33 \text{ mL}^{-1}\text{h}^{-1}$ .

A different phenomenon was observed when 30% (v/v)  $\text{H}_2$  was added to the reactor headspace. In this case, exponential phase of bacterial growth started after 6 h of incubation time but it extended to 24 h where the stationary phase started. The time histories of dry cell concentration and produced hydrogen were presented in Figure 8. Monotonic decreases of microbial growth rate and hydrogen production were observed where hydrogen productivity reduced to  $3.075 \text{ mL}^{-1}\text{h}^{-1}$  when initial substrate concentration in liquid medium was 5 g/L. However, there was no such significant change in growth pattern observed for different substrate concentration in liquid medium.

An extended lag phase in microbial growth was noticed as the quantity initially added  $\text{H}_2$  increased from 30% (v/v) to 40% (v/v). At this condition, the exponential phase commenced at 12 h of incubation time and extended until 27 h. A sharp degradation in microbial growth, as well as biohydrogen production, were also observed (Figure 9). There were no such effects of substrate concentration in liquid medium experience. The hydrogen productivity in this condition was estimated as  $1.54 \text{ mL}^{-1}\text{h}^{-1}$ , which is a sharp alteration compared to 30% (v/v) added  $\text{H}_2$  condition.

Furthermore, when 50% (v/v)  $\text{H}_2$  was added to the reactor headspace, almost no growth condition was observed which is presented in Figure 10. In this case, an extended lag phase with no microbial growth and hydrogen production was seen for 18 h. A short period of exponential phase ended at 27 h was noticed. Almost no hydrogen production condition with productivity of  $0.19 \text{ mL}^{-1}\text{h}^{-1}$  was estimated.

### 3.2. Inhibition Kinetics

In the present investigation, a total of 24 experimental runs were conducted at different initial  $\text{H}_2$  and substrate concentration. Each initially added  $\text{H}_2$  concentration and substrate concentration, and was varied from 2 g/L to 5 g/L. For each combination of  $\text{H}_2$  concentration and substrate concentration, specific growth rate microorganisms were determined. By using Equation (8), plots of  $1/\mu$  and  $1/S$  were obtained at each initially added hydrogen in reactor headspace, which is demonstrated in Figure 11.  $\mu_{\text{max,obs}}$  and  $k_{\text{s,obs}}$  at each headspace  $\text{H}_2$  concentration were determined by evaluating the intercepts and abscissas on Figure 3. The values of  $\mu_{\text{max,obs}}$  and  $k_{\text{s,obs}}$  are provided in the Table 1.

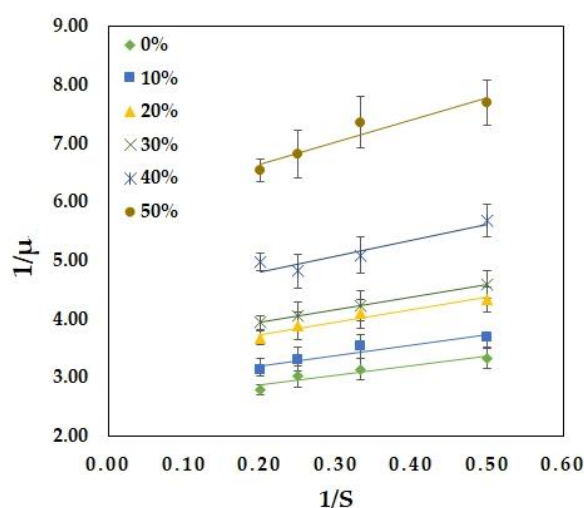


**Figure 11.** Determination of  $\mu_{\max,obs}$  and  $k_{s,obs}$  at different initial concentration of  $H_2$ .

**Table 1.** Values of observed rate constants from experiments.

Initial $H_2$ Concentration in Reactor Headspace ( $v/v$ )	$\mu_{\max,obs}$	$k_{s,obs}$
0%	0.6209	0.6318
10%	0.5523	0.6395
20%	0.4792	0.6285
30%	0.4643	0.6141
40%	0.3695	0.6343
50%	0.2613	0.6521

From Table 1, it can be observed that  $k_{s,obs}$  does not change in any systematic manner with the change of added hydrogen in the reactor headspace. Therefore,  $m = 0$  in Equation (7), which infers the adopted model is a noncompetitive inhibition model and  $k_{s,obs} = k_s$  which will be constant.

After determining values of  $\mu_{\max,obs}$  and  $k_{s,obs}$  at different headspace  $H_2$  concentration, constants in Equation (3) can be evaluated by plotting  $\ln(\mu_{\max,obs})$  vs  $\ln(1-H_2/H_2^*)$  from Equation (9), which is shown in Figure 12. Figure 12 gives the values of  $\mu_{\max}$  and  $n$ . As  $H_2^*$  was not identified from the experiments, a guessed value of 61.5 ( $v/v$ )  $H_2^*$  (24.74 mM) was considered, which gives a straight line with  $R^2 = 0.9823$ . From Figure 12, the intercept and slope give the value of  $\mu_{\max} = 0.976 \text{ h}^{-1}$  and  $n = 0.4786$ .

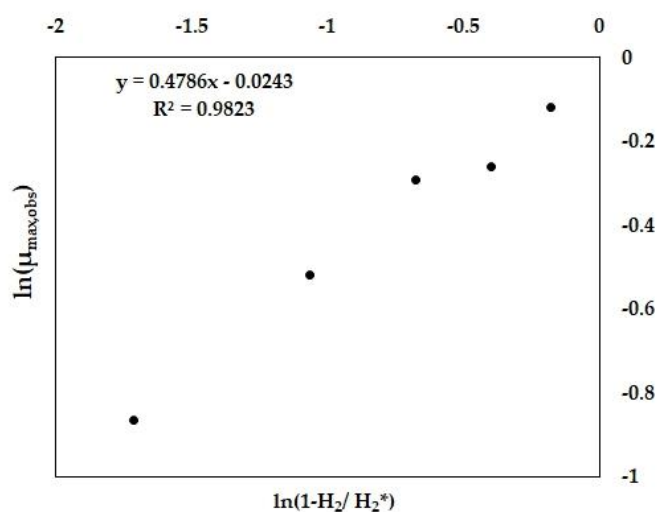


**Figure 12.** Determination of  $\mu_{\max}$ ,  $n$ , and  $H_2^*$  for product inhibition.

#### 4. Discussion

Initially, when there was no hydrogen present in the headspace and the reactor substrate concentration varied from 2 g/L to 5 g/L, the production rates were high and it significantly decreased as the hydrogen concentration increased gradually. When no hydrogen was added to the reactor, the growth phase started after 3 h of incubation time and reached the stationary phase at 21 h. For the 10% added hydrogen condition, the exponential phase started at 6 h and it went until 21 h. On the other hand, when 20% and 30% hydrogen were added, the exponential phase started at 6 h and went until 24 h. Further, when increasing hydrogen concentration by 40% of total headspace, the lag phase elongated by 12 h and the growth phase started at 15 h until 27 h. Almost no growth of bacteria was observed when 50% of the reactor headspace filled with hydrogen. The specific growth rate of biomass decreased as the hydrogen concentration increased in the reactor headspace.

This increased hydrogen concentration reduced the glucose degradation efficiency of bacteria, resulting in a lower hydrogen yield. Hydrogen yield gradually decreased along with specific the growth rate from 1.11 to 0.56 mol/mol.glucose and  $0.621 \pm 0.019 \text{ h}^{-1}$  to  $0.261 \pm 0.021 \text{ h}^{-1}$ , respectively. As the initial hydrogen concentration increases from 0.0 to 0.0161 M, the hydrogen productivity depletion becomes more rapid when the initial hydrogen concentration altered from 0.0161 M to 0.0201 M. Thus, the final partial pressure of hydrogen in the product gas declined and initially added hydrogen concentration increased. The effect of added hydrogen in the reactor on the specific microbial growth rate, final hydrogen concentration and hydrogen yield were calculated by dividing the total amount hydrogen produced by the amount of glucose consumed are summarized in Table 2.

**Table 2.** Effects of added hydrogen on specific growth rate, hydrogen production.

Added Hydrogen (M)/(v/v)	Specific Growth Rate ( $\text{h}^{-1}$ )	Hydrogen Yield (mol- $\text{H}_2$ /mol-glucose)	Final $\text{H}_2$ Partial Pressure (atm)
0.0/(0%)	$0.621 \pm 0.019$	$1.11 \pm 0.0026$	$0.280 \pm 0.015$
$4.023 \times 10^{-3}$ (10%)	$0.552 \pm 0.028$	$1.01 \pm 0.0020$	$0.229 \pm 0.005$
$8.045 \times 10^{-3}$ (20%)	$0.479 \pm 0.029$	$0.92 \pm 0.0022$	$0.214 \pm 0.008$
$1.207 \times 10^{-2}$ (30%)	$0.464 \pm 0.032$	$0.88 \pm 0.0016$	$0.165 \pm 0.013$
$1.610 \times 10^{-2}$ (40%)	$0.369 \pm 0.015$	$0.56 \pm 0.0010$	$0.094 \pm 0.005$
$2.012 \times 10^{-2}$ (50%)	$0.261 \pm 0.021$	$0.21 \pm 0.0010$	$0.0127 \pm 0.003$

From the current study, it is apparent to see that as hydrogen concentration increases in the reactor headspace, it restricts the mass transfer from the liquid to the gaseous phase. Thus, liquid to gas transfer becomes a rate-limiting step that dominates microbial reactions. Consequently, low microbial growth and less hydrogen production occur. On the other hand, hydrogenase, which mobilizes the reversible oxidation of molecular hydrogen, is affected by a high concentration of hydrogen and the process becomes thermodynamically unfavorable for  $\text{H}_2$  formation.

From this analysis, it is clear that the initial addition of hydrogen has a significant impact on microbial growth, hydrogen yield, and hydrogen productivity. As per non-competitive inhibition is concerned, substrate concentration neither influences specific growth rate nor substrate utilization. In order to maintain the hydrogen production at an optimal level, the accumulated hydrogen in reactor headspace should not be more than 8 mMol. It can also be concluded from the present study that when 24.85 mMol hydrogen accumulated in the reactor headspace, reaction stopped and no hydrogen was produced.

#### 5. Conclusions

Growth inhibition caused by hydrogen was examined through the acidogenesis of glucose by a bacterium, *Clostridium acetobutylicum*. Until now, the research showed that the inhibition is caused by  $\text{H}_2$  present in the liquid medium, whereas kinetic models are developed to describe how that inhibition kinetically related to hydrogen production rate but not microbial growth rate. This study

presented the kinetic model that describes how the microbial growth inhibited  $H_2$  in the reactor headspace. The experiments were conducted in a batch reactor to observe the effects of hydrogen accumulated in the reactor headspace on hydrogen production from acidogenesis of glucose by a bacterium, *Clostridium acetobutylicum*. The concluding remarks can be made based on the data of the experiments and prediction of the kinetic model.

A nonlinear and non-competitive inhibition model described the inhibition kinetics of initially added hydrogen concentration on microbial growth and hydrogen production. The maximum specific growth rate ( $\mu_{max}$ ), substrate saturation constant ( $K_s$ ) critical added hydrogen concentration at which microbial growth ceased ( $H_2^*$ ), and degree of inhibition were found to be  $0.976\text{ h}^{-1}$ ,  $0.63 \pm 0.01\text{ g/L}$ ,  $24.74\text{ mM}$ , and  $0.4786$ , respectively. It was observed from the experiment that hydrogen could be an acute inhibitor if allowed to accumulate in reactor headspace. From 10% to 30% ( $v/v$ ) concentration of hydrogen concentration, the microbial growth was decreased linearly. However, as more hydrogen was added in the headspace, microbial activity was inhibited exponentially, particularly after 30% ( $v/v$ ), where there was a potent inhibition in microbial growth and hydrogen production rate. Practically, an extended lag phase in microbial growth and considerably low microbial growth and hydrogen production rate was detected when 50% of total reactor headspace filled with hydrogen. After 61.5% ( $v/v$ ) (i.e.,  $24.74\text{ mM}$ ) of hydrogen accumulated in the reactor, no microbial growth took place and production of hydrogen and microbial growth ceased. Furthermore, different process industries such as biohydrogen and biobutanol production can use the results obtained from the present study for reactor safety and adaptation of control strategies where these kinds of phenomenon occur.

**Author Contributions:** Conceptualization, S.D., R.C. and R.K.C.; Formal analysis, K.N.; Investigation, S.D., R.C. and R.C.; Methodology, R.C. and K.N.; Supervision, R.K.C. and R.C.; Writing—original draft, S.D.; Writing—review & editing, R.C. and F.E.E. All authors have read and agreed to the published version of the manuscript.

**Funding:** The publication charges for this article have been funded by a grant from the publication fund of UiT The Arctic University of Norway.

**Acknowledgments:** The authors wish to thank the Department of Chemical Engineering, Jadavpur University, Kolkata, India, for providing laboratory facilities for this study.

**Conflicts of Interest:** The authors declare no conflict of interest.

## References

1. Offer, G.J.; Howey, D.; Contestabile, M.; Clague, R.; Brandon, N.P. Comparative analysis of battery electric, hydrogen fuel cell and hybrid vehicles in a future sustainable road transport system. *Energy Policy* **2010**, *38*, 24–29. [[CrossRef](#)]
2. Sivagurunathan, P.; Kumar, G.; Bakonyi, P.; Kim, S.H.; Kobayashi, T.; Xu, K.Q.; Lakner, G.; Tóth, G.; Nemestóthy, N.; Bélafi-Bakó, K. A critical review on issues and overcoming strategies for the enhancement of dark fermentative hydrogen production in continuous systems. *Int. J. Hydrog. Energy* **2016**, *41*, 3820–3836. [[CrossRef](#)]
3. Das, D.; Veziroglu, T. Advances in biological hydrogen production processes. *Int. J. Hydrog. Energy* **2008**, *33*, 6046–6057. [[CrossRef](#)]
4. Zhang, T.; Jiang, D.; Zhang, H.; Jing, Y.; Tahir, N.; Zhang, Y. Comparative study on bio-hydrogen production from corn stover: Photo-fermentation, dark-fermentation and dark-photo co-fermentation. *Int. J. Hydrog. Energy* **2020**, *45*, 3807–3814. [[CrossRef](#)]
5. Hay, J.X.W.; Wu, T.Y.; Juan, J.C.; Md. Jahim, J. Biohydrogen production through photo fermentation or dark fermentation using waste as a substrate: Overview, economics, and future prospects of hydrogen usage. *Biofuels Bioprod. Biorefin.* **2013**, *7*, 334–352. [[CrossRef](#)]
6. Eker, S.; Sarp, M. Hydrogen gas production from waste paper by dark fermentation: Effects of initial substrate and biomass concentrations. *Int. J. Hydrog. Energy* **2017**, *42*, 2562–2568. [[CrossRef](#)]
7. Levin, D.B.; Pitt, L.; Love, M. Biohydrogen production: Prospects and limitations to practical application. *Int. J. Hydrog. Energy* **2004**, *29*, 173–185. [[CrossRef](#)]
8. Guo, X.M.; Trably, E.; Latrille, E.; Carrre, H.; Steyer, J.P. Hydrogen production from agricultural waste by dark fermentation: A review. *Int. J. Hydrog. Energy* **2010**, *35*, 10660–10673. [[CrossRef](#)]

9. Oh, S.E.; Zuo, Y.; Zhang, H.; Guiltinan, M.J.; Logan, B.E.; Regan, J.M. Hydrogen production by *Clostridium acetobutylicum* ATCC 824 and megaplasmid-deficient mutant M5 evaluated using a large headspace volume technique. *Int. J. Hydrog. Energy* **2009**, *34*, 9347–9353. [[CrossRef](#)]
10. Logan, B.E.; Oh, S.E.; Kim, I.S.; Van Ginkel, S. Biological hydrogen production measured in batch anaerobic respirometers. *Environ. Sci. Technol.* **2002**, *36*, 2530–2535. [[CrossRef](#)]
11. Chang, S.; Li, J.; Liu, F.; Yu, Z. Effect of different gas releasing methods on anaerobic fermentative hydrogen production in batch cultures. *Front. Environ. Sci. Eng. China* **2012**, *6*, 901–906. [[CrossRef](#)]
12. Esquivel-Elizondo, S.; Chairez, I.; Salgado, E.; Aranda, J.S.; Baquerizo, G.; Garcia-Peña, E.I. Controlled Continuous Bio-Hydrogen Production Using Different Biogas Release Strategies. *Appl. Biochem. Biotechnol.* **2014**, *173*, 1737–1751. [[CrossRef](#)] [[PubMed](#)]
13. Foglia, D.; Wukovits, W.; Friedl, A.; De Vrije, T.; Claassen, P.A.M. Fermentative hydrogen production: Influence of application of mesophilic and thermophilic bacteria on mass and energy balances. *Chem. Eng. Trans.* **2011**, *25*, 815–820.
14. Rafieenia, R.; Pivato, A.; Schievano, A.; Lavagnolo, M.C. Dark fermentation metabolic models to study strategies for hydrogen consumers inhibition. *Bioresour. Technol.* **2018**, *267*, 445–457. [[CrossRef](#)]
15. Kim, D.-H.; Shin, H.-S.; Kim, S.-H. Enhanced H<sub>2</sub> fermentation of organic waste by CO<sub>2</sub> sparging. *Int. J. Hydrog. Energy* **2012**, *37*, 15563–15568. [[CrossRef](#)]
16. Nguyen, T.A.D.; Han, S.J.; Kim, J.P.; Kim, M.S.; Sim, S.J. Hydrogen production of the hyperthermophilic eubacterium, *Thermotoga neapolitana* under N<sub>2</sub> sparging condition. *Bioresour. Technol.* **2010**, *101*, 38–41. [[CrossRef](#)]
17. Saady, N.M.C. Homoacetogenesis during hydrogen production by mixed cultures dark fermentation: Unresolved challenge. *Int. J. Hydrog. Energy* **2013**, *38*, 13172–13191. [[CrossRef](#)]
18. Wang, J.; Wan, W. Kinetic models for fermentative hydrogen production: A review. *Int. J. Hydrog. Energy* **2009**, *34*, 3313–3323. [[CrossRef](#)]
19. Bundhoo, M.A.Z.; Mohee, R. Inhibition of dark fermentative bio-hydrogen production: A review. *Int. J. Hydrog. Energy* **2016**, *41*, 6713–6733. [[CrossRef](#)]
20. Miller, G.L. Use of Dinitrosalicylic Acid Reagent for Determination of Reducing Sugar. *Anal. Chem.* **1959**, *31*, 426–428. [[CrossRef](#)]
21. Han, K.; Levenspiel, O. Extended monod kinetics for substrate, product, and cell inhibition. *Biotechnol. Bioeng.* **1988**, *32*, 430–447. [[CrossRef](#)] [[PubMed](#)]



© 2020 by the authors. Licensee MDPI, Basel, Switzerland. This article is an open access article distributed under the terms and conditions of the Creative Commons Attribution (CC BY) license (<http://creativecommons.org/licenses/by/4.0/>).